Hindawi
Advances in Civil Engineering
Volume 2019, Article ID 3453614, 8 pages
https://doi.org/10.1155/2019/3453614

Research Article

Rockburst Prediction Model Based on Entropy Weight Integrated with Grey Relational BP Neural Network

Yuchao Zheng, Heng Zhong, Yong Fang, Wensheng Zhang, Kai Liu, and Jing Fang

Key Laboratory of Transportation Tunnel Engineering, Ministry of Education, School of Civil Engineering, Southwest Jiaotong University, Chengdu, China

Correspondence should be addressed to Yong Fang; fy980220@swjtu.cn

Received 19 September 2018; Revised 19 March 2019; Accepted 7 April 2019; Published 2 May 2019

Guest Editor: Jian Sun

A rockburst prediction model of the entropy weight grey relational backpropagation (BP) neural network is developed. The model needs to select the evaluation factors according to the engineering practice and establish the sample library. The entropy weight method is used to calculate the objective weight of the characteristic factors, and the similarity between the samples is calculated by the combination of grey relational theory and the entropy method. The training sample of the BP neural network is selected by threshold determination. Finally, we use the trained neural network to estimate the rockburst intensity grade of samples to be tested. This model is applied to the rockburst prediction of Qamchiq tunnel project, and the prediction results are in good agreement with the actual conditions of the subsequent construction, thus verifying the feasibility and effectiveness of the model in the rockburst prediction.

1. Introduction

The increase of cover depth leads to high ground stress and rockburst [1–3]. Rockburst is sudden damage in tunnel excavation because of the transient release of elastic strain energy. Besides, there are many reasons causing rockburst, and the mechanism of rockburst is complex [4–6]. At present, scholars have explained rockburst from the view of energy. However, they focus on partial factors. Due to the limitations of data, some studies cannot get the important information accurately, i.e., in situ stress, geological structure, and rock mechanics parameters [7–9]. The complete rockburst analysis and prediction system are limited in engineering field [10–12]. In the study, the researchers use the help of experimental tunnel to collect data and predict potential rockburst for the constructing tunnel. In order to analyze the large amount of data, the artificial intelligence is employed.

At present, artificial intelligence is widely used to solve nonlinear problems. Backpropagation (BP) neural network, which can learn independently and has good adaptability and antiinterference, has been used to predict the rockburst [13, 14]. However, the defect of BP neural network is that the sample has a great influence on its accuracy. It is easy to cause the weight threshold calculation to fall into local minimum [15, 16]. In order to improve the prediction accuracy, genetic algorithm (GA) [17] and particle swarm optimization (PSO) [18] are applied in the BP neural network to optimize the weight threshold in rockburst prediction.

In order to improve the quality of samples, a prediction model of rockburst intensity is proposed in this study. That is, on the basis of traditional BP neural network, the entropy weight method and grey relational analysis (GRA) are used to optimize the training samples, so as to improve the network generalization accuracy. Further, in the study, the researchers verified the accuracy of this rockburst prediction model through practical engineering application.

Rockburst is influenced by many factors, and the relationship between these factors and rockburst is complicated. It is difficult to find an accurate index to evaluate rockburst. A large amount of field data has proved that there is a certain correlation among the rockbursts [19–21].

The rockburst with the same intensity would occur at conditions with similar factors. So, we filter out some similar series from the field data. It is possible to predict rockbursts at other similar conditions. In order to filter these similar data, we can use the grey relational theory to calculate the correlation of series. The traditional grey relational theory assumes that when the contribution rate of each factor is the same, the weights of each factor would be equal in the calculation of correlation degree [22]. In fact, the influence of different factors on the analysis object is quite different. In order to reflect the influence degree of different evaluation factors, the entropy weight method is used to determine the weight of each factor. Compared with the traditional method, the entropy weight method would make the result more objective and real. Furthermore, we use the BP neural network to predict rockburst intensity in other similar conditions. As a tool of nonlinear multivariate decision making, BP neural network can learn the rules of training samples independently and avoid the interference of human factors. To sum up, it is a feasible way to use the entropy weight method combined with GRA to filter out similar series and predict possible rockburst by BP neural network.

2. Methodology

2.1. Similarity Calculation Method Based on GRA. The GRA is a systematic analysis method which can describe the relation degree between individuals [23]. A grey system means that a system in which part of the information is known and part of the information is unknown. In this system, the attributes of samples expressed are quantified as indexes. We can judge the similarity degree of two samples based on the change trend of these index values. The GRA method is widely used and convenient.

Assume that the system consists of M known series and 1 unknown series and each series has n attribute indexes. So, the unknown series can be expressed as sequence $r_0 = \{r_0(k) \mid k = 1, 2, \ldots, n\}$, and the j-th known series can be expressed as sequence $r_j = \{r_j(k) \mid k = 1, 2, \ldots, n\}$. The details of using GRA to calculate similarity are presented as follows:

Step 1: the dimensions of attribute indexes are not unified; in order to eliminate the influence of dimension, the value of the index is standardized to get its eigenvalue:

$$r_{jk} = \frac{r'_{kj} - \min_j\left(r'_{jk}\right)}{\max_j\left(r'_{jk}\right) - \min_j\left(r'_{jk}\right)}, \tag{1}$$

where r'_{jk} is the value of the k-th attribute of the j-th series and $\max_j(r'_{jk})$ and $\min_j(r'_{jk})$ are the maximum and minimum values of the k-th attribute in all series, respectively.

Step 2: GRA is used to calculate the relation coefficient ξ_{jk} of an attribute between the unknown series r_0 and known series r_j:

$$\xi_{jk} = \frac{\min_j \min_k \left|r_{0k} - r_{jk}\right| + \rho \max_j \max_k \left|r_{0k} - r_{jk}\right|}{\left|r_{0k} - r_{jk}\right| + \rho \max_j \max_k \left|r_{0k} - r_{jk}\right|}, \tag{2}$$

where ρ is the distinguishing coefficient, $\rho \in [0, 1]$, and generally, ρ takes 0.5.

Step 3: the similarity degree s_j between the unknown series and the j-th known series is calculated:

$$s_j = \sum_{k=1}^{n} w_k \xi_{jk}, \tag{3}$$

where w_k is the weight of each attribute index. It is determined by the entropy weight method. The value of s_j reflects the relation degree between known series and unknown series.

2.2. Weight Method Based on Information Entropy. Shannon develops the concept of information entropy to express the randomness [24]. The information entropy describes the reliability, importance, and the weight of an influential factor [25]. In order to avoid the interference of human factors, we use entropy to weight attributes. The entropy of the k-th attribute can be expressed as

$$E_k = \begin{cases} -\ln^{-1}(m) \sum_{j=1}^{m} \frac{r_{jk}}{\sum_{j=1}^{n} r_{jk}} \ln \frac{r_{jk}}{\sum_{j=1}^{n} r_{jk}}, & r_{jk} \neq 0, \\ 0, & r_{jk} = 0, \end{cases} \tag{4}$$

where m is the amount of known series.

And then, the weight of each attribute can be expressed as

$$w_k = \frac{1 - E_k}{n - \sum_{j=1}^{n} E_k}. \tag{5}$$

2.3. Forecasting Method Based on BP Neural Network. BP neural network, which was proposed by Rumelhart and McCelland in 1986, is a multilayer feedforward network trained by error backpropagation algorithm. BP neural network is good at finding out the complex relationship between the factors [26]. BP neural network includes an input layer, an output layer, and one or more hidden layers. BP algorithm is composed of forwarding propagation and backward propagation. If the output layer gets the expected output and the error reaches the expected value, the learning algorithm is finished. Otherwise, the backpropagation is carried out, and it will continue to output after adjusting the weight thresholds between the layers until the output error meets the condition. The standard 3-layer BP neural network model structure is shown in Figure 1.

3. Application in Rockburst Prediction

The researchers applied the proposed prediction model to the Qamchiq tunnel project. The sample library was built

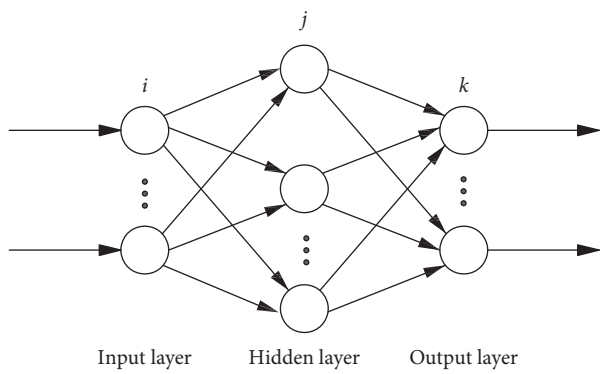

Figure 1: Schematic diagram of BP neural network model.

from the rockburst intensity of the earlier excavated tunnel. The similar sample sequence is filtered out by using the GRA method, and then, the BP neural network is used to infer the rockburst intensity grade of the unexcavated tunnel section. Finally, the results of the calculation will be compared with the actual situation to verify the validity of the model.

3.1. Overview of Qamchiq Tunnel Project. Located in Batisco, Namangan Province, the Federal Republic of Uzbekistan, the Qamchiq tunnel crosses the Kurami Mountains and Kuyinid and Sani Salak Sai River valley. Qamchiq tunnel is a super-long and super-deep buried tunnel with an elevation of 1364 m for entry, 1480 m for the exit; the length of the tunnel is 19.268 km, and the maximum buried depth is about 1275 m. The geography and longitudinal profile is presented in Figure 2. The main lithology of the tunnel site is granite, granodiorite, granite porphyry, syenite porphyry, etc. The surrounding rock is integrated and strong. The groundwater in this area mainly consists of bedrock fissure water, structural fault water, and pore water of quaternary loose rock. The maximum runoff modulus of groundwater is 864 $m^3/d{\cdot}km^2$. The rockburst is a very serious problem during the construction. And, the Qamchiq tunnel is the key project of Anwa electrified railway project. Therefore, it is very necessary to study rockburst prediction in the tunnel site.

The occurrence conditions of rockburst are complex, which are mainly divided into internal causes and external causes. The hard and brittle rock mass under the condition of high geostress accumulates more energy in the geological tectonic movement, and its stress is close to the strength of rock mass, which is the internal cause of rockburst. And, the excavation of the tunnel will disturb the original equilibrium state of surrounding rock, causing the stress redistribution of surrounding rock and the strong stress differentiation of surrounding rock. After the secondary stress concentration reaches the strength of rock mass, the rock mass will collapse and spall. This is the external cause of rockburst. In addition, the development of rock mass structural planes and groundwater will also affect the properties of rock mass energy storage.

Based on the literature investigation and on-the-spot measurement of tunnel, the following indexes are selected to describe a tunnel section [27–33]: the Russian criterion value C_1 ($C_1 = \sigma_{\theta\max}/\sigma_C$, i.e., the ratio of maximum tangential stress of chamber $\sigma_{\theta\max}$ to rock uniaxial compressive strength σ_C), rock brittleness coefficient C_2($C_2 = \sigma_C/\sigma_t$, i.e., ratio of uniaxial compressive strength σ_C to uniaxial tensile strength of rock σ_t), the grade of groundwater condition C_3 and rock integrity coefficient C_4 (Kv value). The above indexes reflect the different attributes of the tunnel section, respectively. C_1 reflects the characteristics of the secondary stress field in the chamber, which is calculated by numerical simulation based on the initial geostress data. C_2 reflects the hardness and brittleness degree of rocks. C_3 reflects the hydrogeological characteristics of the tunnel site, and C_4 reflects the development of the structural plane of the surrounding rock. C_3, the grade of groundwater condition, is evaluated according to the results of a site investigation in tunnel site, and its quantitative results are shown in Table 1. The grade of groundwater condition is negatively correlated with rockburst intensity. When the other conditions are the same, the higher the grade of the groundwater condition, the lower the rockburst intensity.

The rockburst intensity of Qamchiq tunnel was described in four grades: no rockburst (0 grade), slight (1 grade), moderate (2 grade), and severe (3 grade) rockburst. No rockburst means no loosening, breaking of rockburst, or the phenomenon of silent emission. The other main characteristics of the 3 kinds of rockburst are detailed in document [34].

During the tunnel construction, 20 groups of rockburst data were obtained from the tunnel which was constructed earlier. The values of the indexes of the tunnel section are shown in Table 2.

3.2. Calculation of the Weight of Index. The index values are standardized according to formula (1), and then, the weights of each feature attribute are calculated according to formulae (4) and (5). The results are shown in Table 3.

3.3. Calculation of the Similarity Degree of Series. Taking the unexcavated tunnel section MK41 + 425 as an example to show the process of forecasting with this model in detail, the index values of the section are as follows: C_1 is 0.223, C_2 is 8.2, C_3 is 2, and C_4 is 0.75. Then, GRA is used to calculate the similarity between the unknown series and known series 1~20. The similarity degree is calculated by using formulae (2) and (3). The results are shown in Table 4.

As mentioned earlier, the prediction accuracy of BP neural network depends largely on the selection of training samples. If the sample size is too large, the calculation of BP neural network will be trapped in a local minimum, resulting in slow convergence and poor network quality. If the sample size is too small, it cannot fully reflect the impact of indexes on research objective. Therefore, we can consider using fewer high-quality training samples for good model training and finally achieve a higher network generalization accuracy. In this project, the threshold of similarity degree is 0.73 to select a series of BP neural network training samples, which can ensure the fewer number and the high quality of selected samples. The numbers of the selected series are 1, 4, 10, 14, 15, and 20.

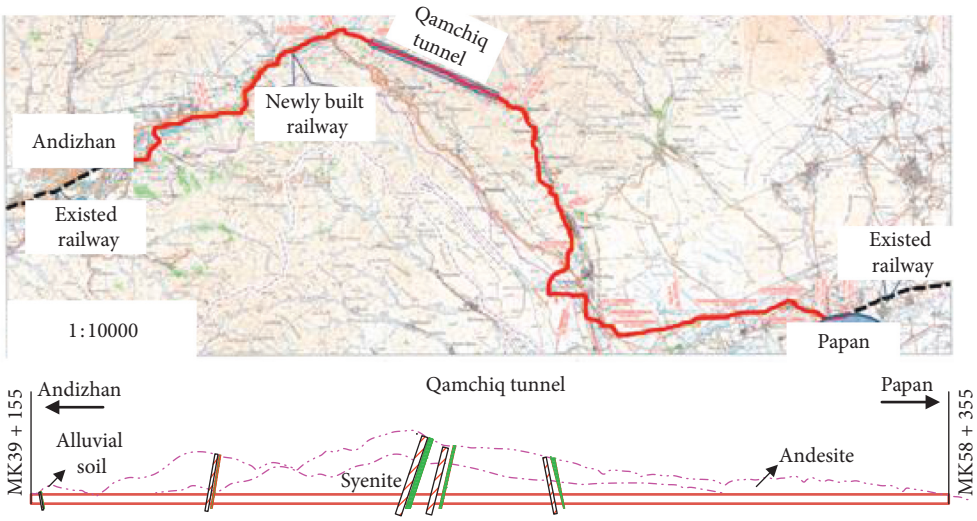

Figure 2: Geography and longitudinal profile of the Qamchiq tunnel.

Table 1: Grade of groundwater condition.

Index	Strongly water rich	Water rich	Weak water rich	Water poor
C_3	1	2	3	4

Table 2: Index information in the sample library.

Series	Tunnel mileage	C_1	C_2	C_3	C_4	Rockburst intensity grade
1	SK39 + 980	0.058	9.3	2	0.54	2
2	SK40 + 800	0.161	11.4	3	0.89	3
3	SK41 + 950	0.166	10.5	3	0.91	3
4	SK42 + 420	0.216	8.6	2	0.76	2
5	SK42 + 980	0.241	4.4	4	0.47	1
6	SK43 + 030	0.225	5.2	4	0.45	1
7	SK43 + 730	0.521	5.5	4	0.37	2
8	SK43 + 780	0.401	3.8	4	0.35	0
9	SK44 + 200	0.439	7.6	4	0.49	2
10	SK44 + 600	0.405	9.8	2	0.52	2
11	SK45 + 380	0.378	8.4	4	0.88	2
12	SK47 + 500	0.58	6.7	4	0.86	3
13	SK47 + 850	0.608	7.0	3	0.74	3
14	SK48 + 950	0.414	8.8	2	0.41	3
15	SK49 + 750	0.446	8.5	2	0.4	3
16	SK53 + 350	0.372	9.7	3	0.92	3
17	SK56 + 300	0.198	6.6	3	0.53	1
18	SK57 + 150	0.147	8.1	3	0.42	1
19	SK57 + 250	0.079	4.2	3	0.39	0
20	SK58 + 310	0.044	5.8	2	0.61	1

Table 3: Entropy weight calculation results.

	C_1	C_2	C_3	C_4
Entropy	0.9173	0.9315	0.8620	0.8805
Weight	0.2024	0.1676	0.3376	0.2924

3.4. Simulation Prediction Using BP Neural Network Model. According to Kosmogorov's theory [35], three-layer feedforward network can approximate any continuous function under the rational conditions, so the network structure of single hidden layer is adopted in this model, which is divided into three layers: a hidden layer, an input layer, and an output layer. The number of hidden layer nodes can be determined by the following empirical formula [36]:

$$h = 2n + 1, \tag{6}$$

where n is the number of input layer nodes. When the number of input layer node takes 4, the number of hidden layers is 9 by formula (6). Using the neural network toolbox function in MATLAB R2016a to train and simulate the network, the BP neural network model is constructed as shown in Figure 3.

In terms of parameter settings, the premnmx function is used to normalize input data, Tansig activation function is used in the process from the input layer to hidden layer, Pureline activation function is used in the process from hidden layer to the output layer, and traingdm function with variable rate gradient descent is used for network training. The initial learning rate is set to 0.01, the training step size is set to 15000, and the global error threshold is set as 1×10^{-5}. For the output layer data, the rockburst grade is expressed by means of unit vector: no rockburst is (1, 0, 0, 0), slight rockburst is (0, 1, 0, 0), medium rockburst is (0, 0, 1, 0), and strong rockburst is (0, 0, 0, 1). Series 1, series 4, series 10, series 14, series 15, and series 20 selected by the GRA method are used as training samples. The variation of global error in the training process is shown in Figure 4. It can be seen from the graph that the neural network achieves convergence after 8637 iterations. The index value of MK41 + 425 tunnel section is input and predicted by the network trained. The result is (0.000, 0.001, 0.999, −0.014). The output data of this section is consistent with the results of 2-grade rockburst. The prediction results determined that the MK41 + 425 tunnel section is grade 2 rockburst.

Referring to the above calculation process of MK41 + 425 tunnel section, we use entropy weight grey relational BP neural network model and traditional BP neural network

Table 4: Similarity degree calculation results.

Series	Similarity degree	Series	Similarity degree	Series	Similarity degree	Series	Similarity degree	Series	Similarity degree
1	0.7636	5	0.5341	9	0.5248	13	0.6642	17	0.6377
2	0.6218	6	0.5496	10	0.7404	14	0.7363	18	0.6270
3	0.6288	7	0.4342	11	0.6032	15	0.7372	19	0.5136
4	0.9692	8	0.4359	12	0.5330	16	0.6045	20	0.7602

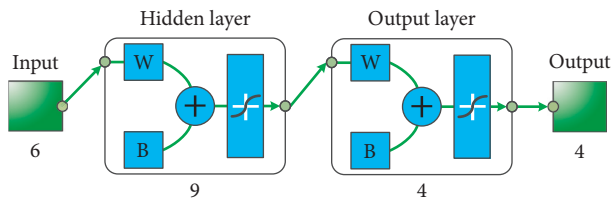

Figure 3: Schematic diagram of the model structure.

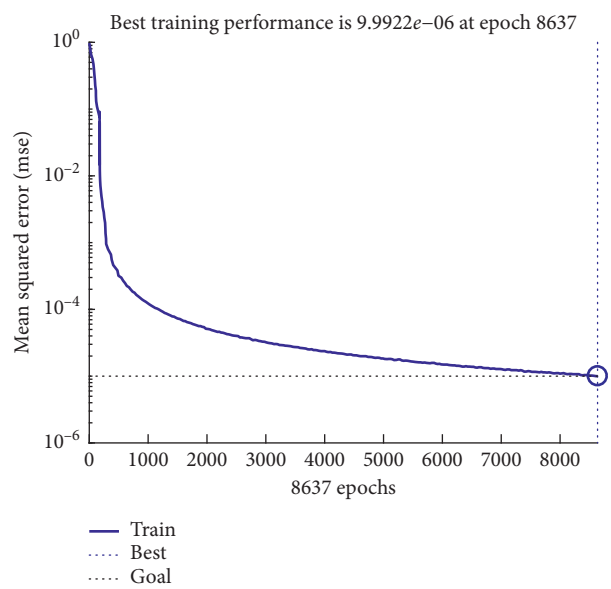

Figure 4: Error curve of entropy weight grey relational BP network training.

model to predict the rockburst intensity grade of the tunnel, respectively, and verify and compare the prediction accuracy of the two methods through follow-up construction. Then, the prediction accuracy of the two methods is compared with the actual situation of subsequent construction. The predicted results corresponding to typical sections of rockburst in actual situations are shown in Table 5. The variation of global error of traditional BP network in the training process is also shown in Figure 5. It can be seen from the graph that the traditional BP network achieves convergence after 28341 iterations. The traditional BP neural network model picks all the 20 groups of rockburst data in the training process without selection. So, it achieves a slower convergence than entropy weight grey relational BP neural network model.

Table 5 shows that the accuracy rate of entropy weight grey relational BP neural network model is 90% while the traditional BP neural network model is only 70%. So, the entropy weight grey relational BP neural network model is more effective than the traditional BP neural network model. It confirms that the filtered high-quality samples can improve the generalization accuracy of BP neural network [37, 38]. Moreover, the prediction results of this model are in good agreement with the actual situation, which basically meets the accuracy requirement of rockburst prediction. A few of the predicted results deviate from the actual situation, which may be due to the complexity and diversity of rockburst genesis in the tunnel site [39, 40]. Besides the four selected indexes, the occurrence of rockburst may also be related to the construction situation, the special structure of the tunnel section, and other reasons, which leads to the deviation between the actual rockburst situation and the law presented by the sample. It shows that the prediction of rockburst should be combined with the monitoring of the construction site. It is necessary to know the dynamic trend of rockburst in time and then formulate corresponding prevention measures [41–44], so as to minimize the loss caused by rockburst.

Table 5: Comparison between simulation prediction results and the actual situation.

Series	Mileage of tunnels	C_1	C_2	C_3	C_4	Traditional BP model	Optimized BP model	Actual situation
1	MK41 + 425	0.223	8.2	2	0.71	2	2	2
2	MK41 + 635	0.171	9.8	3	0.87	1	3	3
3	MK42 + 310	0.230	7.7	2	0.74	2	2	2
4	MK43 + 580	0.548	6.2	4	0.41	2	2	2
5	MK44 + 790	0.391	8.0	4	0.89	2	3	3
6	MK46 + 270	0.446	8.3	4	0.91	3	3	2
7	MK49 + 360	0.537	7.5	2	0.43	3	3	3
8	MK52 + 600	0.388	10.4	3	0.85	3	3	3
9	MK54 + 580	0.206	4.7	3	0.57	1	1	1
10	MK56 + 600	0.188	4.5	4	0.62	1	1	1

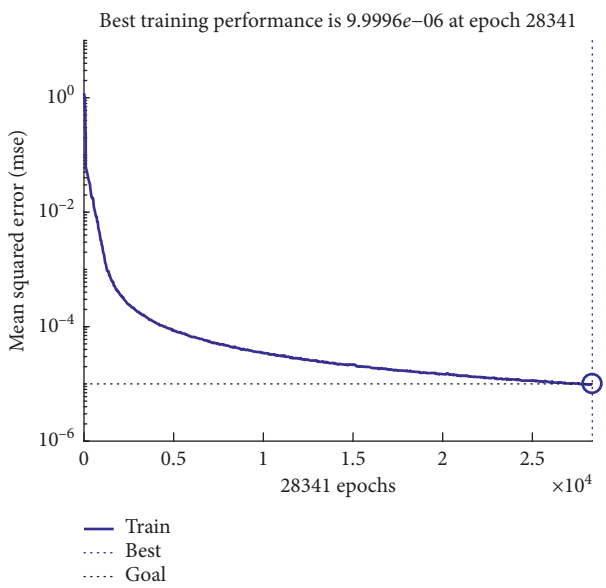

Figure 5: Error curve of traditional BP network training.

4. Conclusions

In this study, entropy weight grey relational BP neural network model is used to predict the rockburst intensity grade of Qamchiq tunnel. The following conclusions are drawn:

(1) The entropy weight grey relational BP neural network model is applied to rockburst prediction for the first time, which provides a new idea and method for tunnel rockburst prediction.

(2) Compared with the traditional BP neural network model, the accuracy of the prediction results of entropy weight grey relational BP neural network model is obviously improved, which confirms that the filtered high-quality samples can effectively improve the generalization accuracy of BP neural network. The whole prediction process is not disturbed by external subjective factors.

(3) The prediction results of the entropy weight grey relational BP neural network model are in good agreement with the actual situation. It met the requirements of rockburst prediction accuracy. After actual engineering verification, the model can be used as a prediction method for rockburst intensity grade.

Data Availability

The data used to support the findings of this study are available from the corresponding author upon request.

Conflicts of Interest

The authors declare that they have no conflicts of interest.

Acknowledgments

This research was supported by the General Program of National Natural Science Foundation of China (51678494) and National Basic Research Program of China (2017YFC0806006).

References

[1] X. Li, Z. Li, E. Wang et al., "Extraction of microseismic waveforms characteristics prior to rock burst using Hilbert-Huang transform," *Measurement*, vol. 91, pp. 101–113, 2016.

[2] J. Qiu, H. Liu, J. Lai, H. Lai, J. Chen, and K. Wang, "Investigating the long-term settlement of a tunnel built over improved loessial foundation soil using jet grouting technique," *Journal of Performance of Constructed Facilities*, vol. 32, no. 5, article 04018066, 15 pages, 2018.

[3] J. Lai, S. He, J. Qiu et al., "Characteristics of seismic disasters and aseismic measures of tunnels in Wenchuan earthquake," *Environmental Earth Sciences*, vol. 76, no. 2, p. 94, 2017.

[4] L. J. Peng, "Deep coal power foundation excavation of rockburst hazard," in *Proceedings of the International Conference on Advanced Engineering Materials and Technology*, vol. 38, pp. 200–203, Guangzhou, China, August 2015.

[5] B. H. Guo, Y. Chen, and P. F. Gou, "Test study on a new rockburst tendency index—yield degree and its influencing factors," in *ISRM Regional Symposium on International Society for Rock Mechanics and Rock Engineering (EUROCK 2014)*, pp. 783–786, Vigo, Spain, May 2014.

[6] Y. Li, S. Xu, H. Liu, E. Ma, and L. Wang, "Displacement and stress characteristics of tunnel foundation in collapsible loess ground reinforced by jet grouting columns," *Advances*

in Civil Engineering, vol. 2018, Article ID 2352174, 16 pages, 2018.

[7] J. Wang, Z. Song, B. Zhao, X. Liu, J. Liu, and J. Lai, "A study on the mechanical behavior and statistical damage constitutive model of sandstone," *Arabian Journal for Science and Engineering*, vol. 43, no. 10, pp. 5179–5192, 2018.

[8] J. L. Qiu, X. L. Wang, J. X. Lai, Q. Zhang, and J. Wang, "Response characteristics and preventions for seismic subsidence of loess in Northwest China," *Natural Hazards*, vol. 92, no. 3, 1909.

[9] Y. Fang, Z. Yao, G. Walton, and Y. Fu, "Liner behavior of a tunnel constructed below a caved zone," *KSCE Journal of Civil Engineering*, vol. 22, no. 10, pp. 4163–4172, 2018.

[10] H. J. Zhang, Z. Z. Wang, F. Lu, G. Y. Xu, and W. G. Qiu, "Analysis of the displacement increment induced by removing temporary linings and corresponding countermeasures," *Tunnelling and Underground Space Technology*, vol. 73, pp. 236–243, 2018.

[11] Z.-Z. Zhang, F. Gao, and X.-J. Shang, "Rock burst proneness prediction by acoustic emission test during rock deformation," *Journal of Central South University*, vol. 21, no. 1, pp. 373–380, 2014.

[12] Q. Wang and H. Sun, "Traffic structure optimization in historic districts based on green transportation and sustainable development concept," *Advances in Civil Engineering*, vol. 2019, Article ID 9196263, 18 pages, 2019.

[13] J. Lai, S. Mao, J. Qiu et al., "Investigation progresses and applications of fractional derivative model in geotechnical engineering," *Mathematical Problems in Engineering*, vol. 2016, Article ID 9183296, 15 pages, 2016.

[14] Y. B. Zhang, Z. Yang, X. L. Yao et al., "Experimental study of rockburst early warning method based on acoustic emission cluster analysis and neural network identification," *Rock and Soil Mechanics*, vol. 38, no. 2, pp. 89–98, 2017.

[15] G. Bo, H. Hejuan, H. Hui et al., "Hybrid PSO-BP neural network approach for wind power forecasting," *International Energy Journal*, vol. 17, no. 4, pp. 211–222, 2017.

[16] V. K. Singh, D. Singh, and T. N. Singh, "Prediction of strength properties of some schistose rocks from petrographic properties using artificial neural networks," *International Journal of Rock Mechanics and Mining Sciences*, vol. 38, no. 2, pp. 269–284, 2001.

[17] Y. H. Peng, K. Peng, J. Zhou, and Z. X. Liu, "Prediction of classification of rock burst risk based on genetic algorithms with SVM," *Applied Mechanics and Materials*, vol. 628, pp. 383–389, 2014.

[18] T. Liu and S. Yin, "An improved particle swarm optimization algorithm used for BP neural network and multimedia courseware evaluation," *Multimedia Tools and Applications*, vol. 76, no. 9, pp. 11961–11974, 2017.

[19] Q. Yan, H. Chen, W. Chen, J. Zhang, S. Ma, and X. Huang, "Dynamic characteristic and fatigue accumulative damage of a cross shield tunnel structure under vibration load," *Shock and Vibration*, vol. 2018, Article ID 9525680, 14 pages, 2018.

[20] Z. Zhang, X. Shi, B. Wang, and H. Li, "Stability of NATM tunnel faces in soft surrounding rocks," *Computers and Geotechnics*, vol. 96, pp. 90–102, 2018.

[21] S. He, L. Su, H. Fan, and R. Ren, "Methane explosion accidents of tunnels in SW China," *Geomatics, Natural Hazards and Risk*, vol. 10, no. 1, pp. 667–677, 2018.

[22] H. Jun, J. Dong, K. Wang et al., "Research on CPSO-BP model of slope stability," *Rock and Soil Mechanics*, vol. 37, pp. 577–582, 2016.

[23] G. Kim, Y. Jong, and S. F. Liu, "Generalized hybrid grey relation method for multiple attribute mixed type decision making," *Journal of Grey System*, vol. 26, no. 2, pp. 142–153, 2014.

[24] C. E. Shannon, "Prediction and entropy of printed English," *Bell System Technical Journal*, vol. 30, no. 1, pp. 50–64, 1951.

[25] M. Kelbert, I. Stuhl, and Y. Suhov, "Weighted entropy: basic inequalities," *Modern Stochastics: Theory and Applications*, vol. 4, no. 3, pp. 233–252, 2017.

[26] Y. Zhao, "Research and application on improved BP neural network algorithm," in *Proceedings of the 2010 5th IEEE Conference on Industrial Electronics and Applications*, Taichung, Taiwan, June 2010.

[27] M. Ji, H. J. Guo, Y. D. Zhang, T. Li, and L.-S. Gao, "Hierarchic analysis method to evaluate rockburst risk," *Mathematical Problems in Engineering*, vol. 2015, Article ID 184398, 8 pages, 2015.

[28] J. Qiu, X. Wang, S. He, H. Liu, J. Lai, and L. Wang, "The catastrophic landside in Maoxian county, Sichuan, SW China, on June 24, 2017," *Natural Hazards*, vol. 89, no. 3, pp. 1485–1493, 2017.

[29] W. Shen, L. M. Dou, H. He et al., "Rockburst assessment in multi-seam mining: a case study," *Arabian Journal of Geosciences*, vol. 10, no. 8, 2017.

[30] J. Lai, X. Wang, J. Qiu, J. Chen, Z. HU, and H. Wang, "Extreme deformation characteristics and countermeasures for a tunnel in difficult grounds in southern Shaanxi, China," *Environmental Earth Sciences*, vol. 77, no. 19, p. 706, 2018.

[31] R. Ren, S. Xu, Z. Ren et al., "Numerical investigation of particle concentration distribution characteristics in twin-tunnel complementary ventilation system," *Mathematical Problems in Engineering*, vol. 2018, Article ID 1329187, 13 pages, 2018.

[32] R. Ren, H. Zhou, Z. Hu, S. He, and X. Wang, "Statistical analysis of fire accidents in Chinese highway tunnels 2000–2016," *Tunnelling and Underground Space Technology*, vol. 83, pp. 452–460, 2019.

[33] K. G. Sun, W. P. Xu, W. G. Qiu, H. B. Li, Q. Y. Xian, and T. Li, "Study on the characteristics of safety distribution changing with buried depth for metro station in upper-soft and lower-hard stratum," *Advances in Civil Engineering*, vol. 2018, Article ID 6047919, 14 pages, 2018.

[34] W. Deng, C. Y. Liu, H. J. Li et al., "Mechanism of rockburst of Qamchiq tunnel in Uzbekistan," *Tunnel Construction*, vol. 36, no. 3, pp. 275–281, 2016, in Chinese.

[35] S. Haykin, *Neural Networks: A Comprehensive Foundation*, Prentice Hall, Upper Saddle River, NJ, USA, 1994.

[36] X. F. Li, S. Y. Xiang, P. F. Zhu, and M. Wu, "Establishing a dynamic self-adaptation learning algorithm of the BP neural network and its applications," *International Journal of Bifurcation and Chaos*, vol. 25, no. 14, article 1540030, 2015.

[37] W.-Y. Guo, T.-B. Zhao, Y.-L. Tan, F.-H. Yu, S.-C. Hu, and F.-Q. Yang, "Progressive mitigation method of rock bursts under complicated geological conditions," *International Journal of Rock Mechanics and Mining Sciences*, vol. 96, pp. 11–22, 2017.

[38] Z. Zhang, H. Zhang, Y. Tan, and H. Yang, "Natural wind utilization in the vertical shaft of a super-long highway tunnel and its energy saving effect," *Building and Environment*, vol. 145, pp. 140–152, 2018.

[39] Z.-F. Wang, W.-C. Cheng, and Y.-Q. Wang, "Investigation into geohazards during urbanization process of Xi'an,

China," *Natural Hazards*, vol. 92, no. 3, pp. 1937–1953, 2018.

[40] J. Lai, K. Wang, J. Qiu, F. Niu, J. Wang, and J. Chen, "Vibration response characteristics of the cross tunnel structure," *Shock and Vibration*, vol. 2016, Article ID 9524206, 16 pages, 2016.

[41] R. Ren, D. Yu, L. Wang, K. Wang, H. Wang, and S. He, "Typhoon triggered operation tunnel debris flow disaster in coastal areas of SE China," *Geomatics, Natural Hazards and Risk*, vol. 10, no. 1, pp. 562–575, 2018.

[42] J. Qiu, T. Yang, X. Wang, and G. Zhang, "Review of the flame retardancy on highway tunnel asphalt pavement," *Construction and Building Materials*, vol. 195, pp. 468–482, 2019.

[43] Y. Fang, Z. Chen, L. Tao, J. Cui, and Q. Yan, "Model tests on longitudinal surface settlement caused by shield tunnelling in sandy soil," *Sustainable Cities and Society*, vol. 47, article 101504, 2019.

[44] J. Lai, J. Qiu, H. Fan et al., "Fiber bragg grating sensors-based in-situ monitoring and safety assessment of loess tunnel," *Journal of Sensors*, vol. 2016, Article ID 8658290, 10 pages, 2016.